Chemical Engineering Journal 485 (2024) 149824

Contents lists available at ScienceDirect

Chemical Engineering Journal

journal homepage: www.elsevier.com/locate/cej

From microbial heterogeneity to evolutionary insights: A strain-resolved metagenomic study of H_2S-induced changes in anaerobic biofilms

Gabriele Ghiotto [1,a], Nicola De Bernardini [1,a], Ginevra Giangeri [b], Panagiotis Tsapekos [b], Maria Gaspari [c], Panagiotis G. Kougias [c], Stefano Campanaro [a,*], Irini Angelidaki [b], Laura Treu [a]

[a] Department of Biology, University of Padova, Via U. Bassi 58/b, 35121 Padova, Italy
[b] Department of Chemical and Biochemical Engineering, Technical University of Denmark, Kgs. Lyngby DK-2800, Denmark
[c] Soil and Water Resources Institute, Hellenic Agricultural Organization - Dimitra, Thermi, Thessaloniki 57001, Greece

ARTICLE INFO

Keywords:
Carbon dioxide
Methanogenesis
Hydrogen sulfide
Metagenomics
Strain deconvolution
Single nucleotide variants

ABSTRACT

The hidden layers of genomic diversity in microbiota of biotechnological interest have been only partially explored and a deeper investigation that overcome species level resolution is needed. CO_2-fixating microbiota are prone to such evaluation as case study. A lab-scale trickle-bed reactor was employed to successfully achieve simultaneous biomethanation and desulfurization on artificial biogas and sulfur-rich biogas, and oxygen supplementation was also implemented. Under microaerophilic conditions, hydrogen sulfide removal efficiency of 81% and methane content of 95% were achieved. *Methanobacterium* sp. DTU45 emerged as predominant, and its metabolic function was tied to community-wide dynamics in sulfur catabolism. Genomic evolution was investigated in Gammaproteobacteria sp. DTU53, identified as the main contributor to microaerophilic desulfurization. Positive selection of variants in the hydrogen sulfide oxidation pathway was discovered and amino acid variants were localized on the sulfide entrance channel for sulfide:quinone oxidoreductase. Upon oxygen supplementation strain selection was the primary mechanism driving microbial adaptation, rather than a shift in species dominance. Selective pressure determined the emergence of new strains for example on Gammaproteobacteria sp. DTU53, providing in depth evidence of functional redundancy within the microbiome.

1. Introduction

The urgent need to mitigate the greenhouse effect has prompted extensive research into sustainable approaches for reducing carbon dioxide (CO_2) emissions. Biological biogas upgrading involves the transformation of CO_2 present in biogas streams into methane (CH_4) through microbial-driven processes [1]. The inherent metabolic capabilities of anaerobic microbiomes offer an environmentally friendly and cost-effective alternative to conventional chemical biogas upgrading methods [1]. However, inhibitory compounds, such as hydrogen sulfide (H_2S), pose a significant challenge to the successful implementation of the upgrading process. H_2S, known for its corrosive and toxic properties even at low ppm, can exert detrimental effects on microbiota, leading to system instability [2]. A solution to boost H_2S removal is the injection of a small amount of air (2–8 % v/v) which has demonstrated promising outcomes [3]. This strategy facilitates the oxidation of gaseous H_2S, resulting in the formation of either free sulfur or sulfurous acid through spontaneous reactions according to equations (1) and (4). The chemical catalysis can be combined with biological desulfurization, a process based on biotic conversion of H_2S to diverse sulfur compounds, such as elemental sulfur, sulfate and reactive sulfur species [4–6]. The biotic H_2S oxidation is catalyzed by sulfur-oxidizing bacteria (SOB), through a mechanism not yet completely clarified [7]. In strictly anoxic conditions SOB use nitrate or manganese as the terminal electron acceptors for either complete or incomplete oxidation of H_2S to sulfate or elemental sulfur, respectively [8,9]. Moreover, SOB belonging to the genus *Thiobacillus* and *Beggiatoa* can oxidize H_2S to sulfate while performing aerobic respiration [4], thus using oxygen (O_2) as final electron acceptor according to equations (1)-(3) [3]. A recent study has already evidenced excellent H_2S removal efficiency, driving enhanced production and recovery of S^0 [10]. The high abundance and activity of species related to *Thiomicrospiraceae* and *Burkholderiaceae* indicated potential mechanisms

Abbreviations: CO_2, Carbon dioxide; TBR, Trickle-bed reactor; SOB, Sulfur-oxidizing bacteria; SNVs, Single-nucleotide variants.

* Corresponding author.
E-mail address: stefano.campanaro@unipd.it (S. Campanaro).

[1] These authors have contributed equally to this work.

https://doi.org/10.1016/j.cej.2024.149824
Received 25 October 2023; Received in revised form 14 February 2024; Accepted 17 February 2024
Available online 21 February 2024

for tolerance to sulfide inhibitory effects and resistance to sulfide-induced respiratory inhibition [10].

$$H_2S + \frac{1}{2}O_2 \rightarrow S^0 + H_2O \ \Delta G^\circ = -209.4kJ/reaction \quad (1)$$

$$H_2S + H_2O + \frac{3}{2}O_2 \rightarrow H_2SO_4 \ \Delta G^\circ = -587.1kJ/reaction \quad (2)$$

$$H_2S + 2O_2 \rightarrow H_2SO_4 \ \Delta G^\circ = -798.2kJ/reaction \quad (3)$$

$$2H_2S + 3O_2 \rightarrow 2H_2SO_3 \ \Delta G^\circ = -129.5kJ/reaction \quad (4)$$

A comprehensive understanding of the molecular-level effects of H_2S in complex microbial communities is essential for devising effective mitigation strategies. The interplay between microbes and their adaptive responses to varying gas streams, particularly under microaerophilic conditions, can significantly influence H_2S removal rates [3]. Gaining insights into the interactions between key players driving CH_4 production and sulfur-oxidizing species is crucial. This information would elucidate the underlying mechanisms governing microbiota and the biogas production process. Additionally, an investigation of adaptive strategies employed by microbes, even at strain level, in the presence of H_2S can shed light on the potential development of resilient microbial communities. Previous studies already suggested that newly emerging strains can withstand inhibitory conditions and ensure stable bioconversion [11,12]. Alas, combining methanation with desulfurization in microaerophilic conditions requires a delicate balance to prevent inhibitory O_2 levels for the methanogens [13].

Notwithstanding this contingency, when microorganisms are exposed to a severe selective pressure such as increasing concentrations of a toxicant, including H_2S or O_2, mutations are occurring in their genome. Genetic variants providing a survival advantage are positively selected and can lead to the development of resistance mechanisms. Previous studies overlooked microbial mutations that lead to variations in dominant strains, especially when the microbiome is exposed to a long acclimatization period [14]. Moreover, despite the significant role of genomic heterogeneity in the anaerobic microbiome and the impact of environmental factors on microbial resilience and evolutionary dynamics [15], the main exploration was in the human gut [11]. The significance of variants and their role in microbial adaptation, particularly in response to different environmental stressors, like the coexistence of methanogens and SOB during H_2S oxidation, remains largely unexplored. Delving deeper into strain-level dynamics, including emerging mutations, is crucial for a comprehensive understanding of this phenomenon.

Here the evolution of microbial dynamics of a mixed-methanogenic culture in response to exposure at high H_2S levels in a trickle-bed reactor (TBR) was investigated. The coupling of biomethanation and desulfurization was tested in anoxic and microaerophilic conditions. Packing material was used to facilitate the development of the microbiota in the form of biofilm. The microbiota evolution under prolonged exposure to high H_2S concentrations was explored using strain-resolved metagenomics, combining variant calling and strain deconvolution in a pioneering way. The first allowed tracing the strains by identifying distinct patterns of alleles across single nucleotide variants (SNVs) [16], while the second employed statistics to extract strain genotypes, relying on allele frequencies [17]. This integrated analysis provided novel insights into fine-scale evolutionary mechanisms operating within a complex microbiome. Specifically, the identified mutations in the primary SOB were among the main drivers for the observed shift in dominance following the introduction of air by improving the fitness of one of the detected strains. This acquired phenotypic advantage enabled the evolved strain to outperform its competitor and thrive more effectively over time. The comprehensive approach utilized in the current study shed light on the selection of resistant microorganisms and contributed to a deeper understanding of microbial adaptive strategies.

2. Materials and methods

2.1. Characteristics and operation of the lab-scale TBR

The gas-tight TBR made of glass column with a height of 51 cm and a packed working volume of 0.8 L was operated at thermophilic conditions (54 ± 1 °C). The TBR was filled with a mixture of polyethylene Raschig rings (PE08, Tongxiang Small Boss Special Plastic Products ltd) with a dimension of 7 mm × 10 mm and surface area of 3500 m^2/m^3 for each piece and polypropylene/polyethylene rings (BioFLO 9-Smoky Mountain Bio Media, USA) with a density of 1 $g \bullet cm^{-3}$ and a surface area of 800 $m^2 \bullet m^{-3}$. The gas retention time (GRT) was kept constant at 4.0 h and the inlet gas flow rate was set at 6 $L \cdot Lr - 1 \cdot day - 1$ using a peristaltic pump. The experiment was conducted at distinctly different periods based on the CO_2 source. All the used feeding mixtures contained about 23 % CH_4, 15 % CO_2, and 62 % H_2 and were prepared to obtain a stoichiometric H_2/CO_2 ratio of 4:1. In phase S1 the used gasses were pure and collected from gas cylinder (Air Liquide, Danmark A/S). After achieving steady CH_4 content above 90 % for about 8 days the feeding mixture (phase S2) was modified combining pure H_2 (Air Liquide, Danmark A/S) with biogas collected from a lab-scale continuously stirred tank reactor (CSTR). The biogas had a composition of 60 ± 3 % CH_4 and 40 ± 3 % CO_2 and was produced under SO_4^{2-}-rich conditions, resulting in an average H_2S concentration of 2962 ± 84 ppm. After achieving CH_4 content above 85 % for 5 days the gas feeding strategy passed to phase S3. Air (0.009 % v/v) was added to the mixture used in phase S2 to achieve microaerophilic conditions with 0.002 % v/v O_2. The gas was supplied in concurrent flow with digestate collected from a manure-based CSTR that was used as a nutrients source. The TBRs was inoculated with a thermophilic inoculum previously described with the following characteristics: pH 8.6, total solids 1.80 ± 0.01 % (w/w), volatile solids 0.80 ± 0.01 % (w/w), total ammonia nitrogen (TAN) 687.01 ± 13.51 mg NH_4^+-N/L, and volatile fatty acids (VFAs) 99.01 ± 7.41 mg/L. The digestate was pasteurized before usage and trickled at a constant flow rate of 20 $mL \cdot Lr^{-1} \cdot min^{-1}$ [14]. Moreover, to provide necessary moisture for the packing materials and ensure that the methanogenic microbes had access to the nutrients, the TBR was flooded twice per week with liquid volume from the sump.

2.2. Analytical methods

The total outlet gas was measured using a water displacement gas-counting. The gas composition over the TBR height was analyzed using a gas chromatograph (GC-TRACE 1310, Thermo Fisher Scientific, US) equipped with a thermal conductivity detector (TCD) and Thermo (P/N 26004–6030) Column (30 m length, 0.320 mm inner diameter, and film thickness 10 μm) with helium as carrier gas. VFAs concentrations were measured by gas chromatography (Agilent 7890A gas chromatograph, Agilent Technologies, US) equipped with a flame ionization detector (FID) and SGE capillary column (30 m length, 0.53 mm inner diameter, film thickness 1.00 μm) with helium as carrier gas. The injector and detector temperatures were 150 °C and 220 °C, respectively. The initial temperature of the column oven was held at 45 °C for 3.5 min, then increased to 210 °C at a ramping rate of 15 °C/min, and then held for 4 min at 210 °C. All samples were analyzed in duplicate. pH was monitored with a FiveEasy Plus Benchtop FP20 (Mettler Toledo, CH). H_2S in the inlet and outlet gas mixtures was measured with Geotech BIOGAS 5000 portable gas monitor (QED Environmental Systems 206 Ltd., UK).

2.3. Microbial sampling and DNA extraction

The effect of different feeding mixture composition on the microbial community was assessed collecting DNA samples from two sampling ports through the TBR height. Two samples, one per sampling point, were collected from packing material located in the top and middle

section. The DNA extraction was performed at the end of each period, respectively day 25, 68 and 79 of the experiment resulting in six samples. The extraction of genomic DNA was carried out using a modified version of the DNeasy PowerSoil® protocol (QIAGEN GmbH, Hilden, Germany), as described in a previous study [18]. To enhance the purity of the nucleic acids obtained, an initial cleaning step was performed using Phenol, Chloroform, and Isoamyl Alcohol (in a 25:24:1 ratio). To ensure the quality and concentration of the extracted DNA, NanoDrop spectrophotometer (Thermo Fisher Scientific, Waltham, MA, USA) and Qubit 2.0 fluorometer (Thermo Fisher Scientific, Waltham, MA, USA) were used.

2.4. Metagenomic sequencing and binning results

The sequencing strategy was based on the NovaSeq 6000 platform (Illumina Inc., San Diego CA). Library preparation was conducted using Nextera DNA Flex Library Prep Kit (Illumina Inc., San Diego CA) at the Biology Department sequencing facility (University of Padova, Italy) and sequenced with Illumina NovaSeq 6000 platform (2 × 150, paired end). Raw sequences have been submitted to the Sequence Read Archive (NCBI) under the project PRJNA972863.

Bioinformatics analysis of NGS data was performed using a genome-centric metagenomics approach, as previously described [19]. Reads were filtered with Trimmomatic v0.39 [20] to remove adapters and low-quality bases, and checked for contamination with the BBDuck (v38.93) tool. Resulting reads were assembled using MegaHit (v1.2.9) [21], selecting the "*meta*-sensitive" option and ignoring all contigs shorter than 1 kbp. A combination of tools was used to perform the binning analysis [19] and Bowtie2 (v2.4.5) [22] were used to generate the coverage profiles. CheckM2 (v1.0.1) [23] was used to assess the quality of the metagenome assembled genomes (MAGs). MAGs were filtered, de-replicated and aggregated using DAStool (v1.1.5) [24]. Lastly, recovered MAGs were classified into high, medium and low quality according to the minimum information about metagenome-assembled genome guidelines (MIMAG) [25]. High and medium quality MAGs are available at link (https://doi.org/10.6084/m9.figshare.24958812). GTDB-Tk (v2.1.0) [26] was used for taxonomic classification. Identifiers were assigned to the MAGs based on taxonomic level and a progressive number was also included in the final name. The phylogenetic tree was generated using PhyloPhlAn 3.0 (v3.0.2) [27] and drawn with iTOL [28].

2.5. Statistics and functional analysis

Further statistics and functional analysis took into consideration only high quality MAGs [25]. CoverM (v0.6.1) [29] was used to retrieve MAGs's relative abundance and read counts. Prodigal (v2.6.3) [30] was used for gene prediction, while functional annotation was done with eggNOG-mapper (v2.1.9) [31]. The reference database used was the Kyoto Encyclopedia of Genes and Genomes (KEGG) [32], consulted for enzyme class, orthology and metabolic pathways. The KEGG orthologs obtained from the gene annotations were used to identify genes associated with sulfur metabolism in the MAGs. Pathway's completeness was assessed based on manual revision for sulfur related metabolisms whereas general functional trait profile was determined with Microbe-Annotator (v2.0.4) [33]. Out of all the annotated pathways, only results relevant for biogas production were visualized as heatmap (**Supplementary Fig.S2**). SNVs analysis was performed using the software InStrain (v1.6.3) [16] on the high quality MAGs recovered. MAGs with RA above 2 % were selected based on variant metrics, and a strain deconvolution pipeline was applied using STRONG [17]. The abundances of the deconvoluted strains were defined taking into account the relative abundance of the corresponding MAG. A variant phasing approach was performed by clustering the SNVs frequency and then comparing this information with the relative abundance of predicted strains, as previously described [34]. This procedure allowed to group together SNVs most probably belonging to the same strain, enabling to track the transmission of genetic modifications over time. Lastly, the proteins affected by SNVs were modeled with AlphaFold [35,36] to obtain the 3D structure of the mutated polypeptides and compare them with the original ones. Moreover, the sequence of the proteins were aligned using the multiple sequence alignment tool Clustal Omega, based on the ClustalW algorithm [37], against reference structure deposited in Swiss-Prot. This comparison allowed us to evaluate the potential impact of the SNVs on the investigated protein.

3. Results

3.1. Evolution of anaerobic microbiome under increasing complexity of gas phase and microaerophilic condition

A genome-centric metagenomic approach was used to explore the evolving structure of the complex methanogenic consortium in three timepoints, one per each stage (S1- artificial biogas, sulfur-rich biogas S2- without and S3- with O_2), and in two sampling points at different heights of the TBR (Top and Middle) per each timepoint. Additionally, the gradient of operational conditions present across the axial direction of the TBR was investigated. The focus was on the crucial effect of the downward decreasing CO_2 and H_2 partial pressure on biofilm development and microbial competition [38]. A total of 146 MAGs were recovered, of which 97 classified as high quality [25] (**Supplementary Table S1**). The microbiome was stratified into eleven distinct phyla and dominated across all samples by *Methanobacterium* sp. DTU45, the only representative of the archaea domain and a known hydrogenotrophic methanogen [39]. This species has previously demonstrated to be exceptionally well-fitted for artificial vessel ecosystems, regardless of the diverse experimental condition tested (ANI > 99.6 % with respect to *Methanobacterium* DTU-pt_142 and *Methanobacterium* DTU-pt_46) [38,40]. Additionally, it has already been reported to be capable of interspecies electron transfer with the bacterial population during the carbon fixation metabolism [41]. Further attention was posed to the microbiome dominant fraction including a total of 38 species collectively representing 77 % to 87 % of the total microbiome (Fig. 1).

After the first 12 days of operation, the microbiota consumed constantly the substrate resulting in the almost total absence of CO_2 and H_2 in the effluent gas. Total VFA levels showed a fluctuating pattern with an average value of 222 mg/L (Fig. 2). Acetate was accounting for more than 97 % of the total VFA, indicating that species performing homoacetogenic metabolism were competing for resources, reducing the final CH_4 production rate. However, in the last 6 days of S1, complete methanation was achieved (CH_4 content ~ 98 %, Fig. 2), thus indicating that the hydrogenotrophic archaeon was winning the competition for the carbon sources (**Supplementary Table S2**).

The establishment of a multi-trophic community was favored by the shift from artificial (stage 1, S1) to H_2S-rich (stage 2, S2) biogas stream, which provided an increased variety of substrates (**Supplementary Fig. S2**). During S2 the gaseous feed heavily affected the microbiota metabolism, drastically decreasing the abundance of hydrogen-oxidizing bacteria. These potentially redirect electrons from H_2 to the sulfate-sulfur assimilatory pathway and influence positively putative SOB species, such as Gammaproteobacteria sp. DTU53. The new feeding condition induced consumption of the main substrates that deviated from the typical 1:4 ratio of the stoichiometry for hydrogenotrophic methanogenesis [1].

From day 56 the culture acclimatized and gradually recovered its full methanogenic activity. The progressive consumption of VFA experienced in S2 highlighted a reduced acetogenic activity with respect to overall acetate oxidation, as it is known that homoacetogens are sensitive to H_2S concentration higher than 450 ppm [42]. The third stage (S3) started on day 69 and was interrupted after ten days of stable CH_4 biogenesis (95 % ± 2 %, Fig. 2).

The addition of air to the gas mixture provided in S3 further shaped

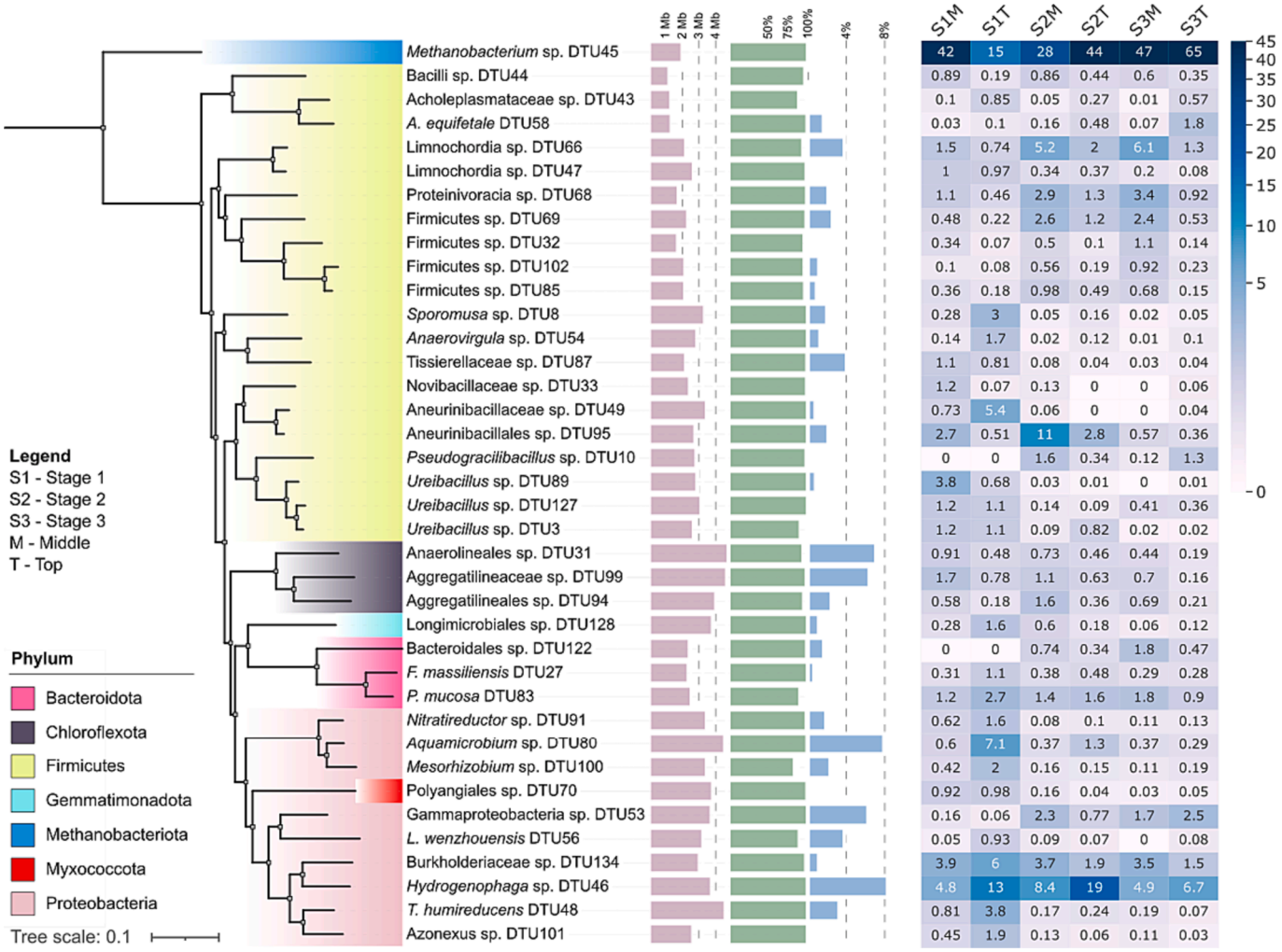

Fig. 1. Phylogenetic tree and relative abundance of the species. From left to right tree showing phylogenetic relationships, barplots reporting genome size, contamination, and completeness, and heatmap representing relative abundance of species per sample. MAGs are depicted only if passing a minimum threshold of relative abundance set at 0.85% in at least one sample. Samples are organized according to the sampling point location (Middle or Top), and the stage of the experiment (S1, S2, S3).

the microbial community, favoring the growth of potentially oxygen-tolerant species, such as Gammaproteobacteria sp. DTU53, and facultative anaerobes, like *A. equifetale* DTU58 [43]. Indeed, in S3 more than 81 % of the initial H_2S content (3011 ppm) was removed, reaching a final concentration of 559 ppm. In recent microaeration studies members of Proteobacteria phylum displayed some tolerance to O_2 exposure [44,45], thus providing a possible explanation for the observed fitness of Gammaproteobacteria sp. DTU53. According to gene annotation, this bacterium contains genes (eg. *Cox*, *Sdh*) associated with the five complexes of the aerobic respiratory chain present in facultative anaerobes (**Supplementary Table S3**). When microaerophilic conditions were induced in S3, Gammaproteobacteria sp. DTU53 could potentially undergo metabolic reprogramming, facilitating the transition from fermentation to aerobic respiration. Remarkably, *Methanobacterium* sp. DTU45 also appeared to be affected by the changed feeding mixture, as its relative abundance reached its maximum. The higher resistance of *Methanobacterium* sp. DTU45 relies on its biofilm formation capability, which could hypothetically provide better protection against toxic agents, such as O_2 [46]. In conclusion, the microbiota thrived in high H_2S concentrations, showing strong H_2S-oxidizing activity, uniform biofilm formation, and stable methanogenesis under anaerobic and microaerophilic conditions.

3.2. Functional annotation of EPS secretion systems and sulfur compounds metabolism

A molecular-level investigation is needed to confirm the adaptive responses of the microcosm to varying gas stream compositions. Therefore, identifying the microbes responsible for maintaining stable biomethanation and efficient H_2S removal becomes pivotal to reveal the adaptive strategies at strain resolution. Three main metabolic routes were chosen: a) the biofilm formation, responsible for the favorable growth environment, b) the Wood–Ljungdahl (WL) pathway, employed by syntrophic acetate oxidizing bacteria (SAOB) to fuel the methanogenesis, and c) the H_2S catabolism.

First, the metagenome was scouted for the presence of extracellular polymeric substances (EPS) secretion system to investigate the species contributing to biofilm development. A set of genes involved in capsular polysaccharide synthesis and sugar transfer (*cpsG*, *cpsM*, *cpsO*), responsible for the secretion of EPS was found in the archaeal MAG. Additionally, highly abundant bacteria such as *Hydrogenophaga* sp. DTU46 and Gammaproteobacteria sp. DTU53 encoded for over 20 genes related to biofilm formation as well (**Supplementary Table S4**).

Second, none of the abundant MAGs encode for the entire gene set of the canonical WL pathway. Nevertheless, 24 MAGs possess the formate-tetrahydrofolate ligase (*fhs)* gene, a molecular marker for potential

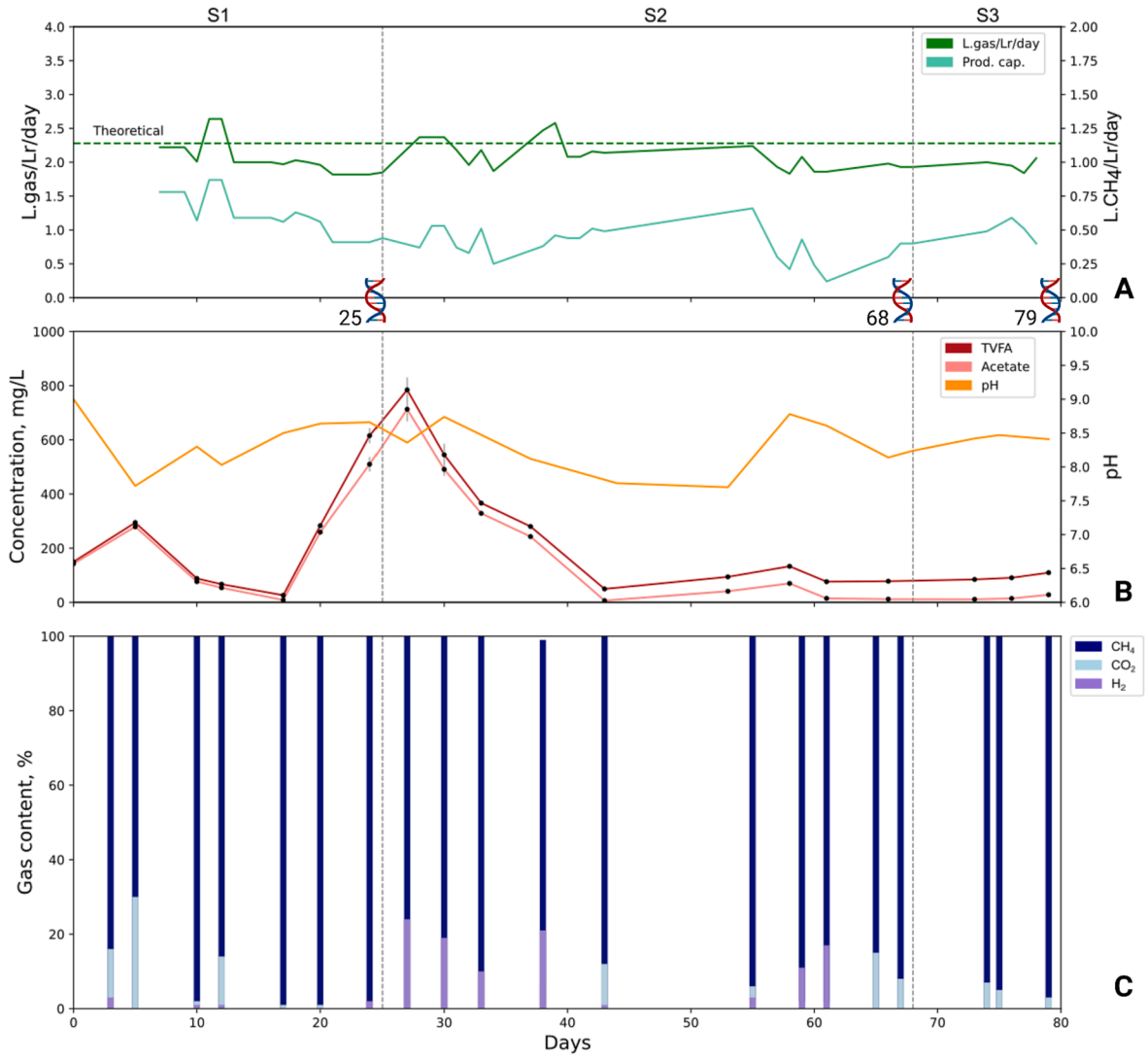

Fig. 2. Biomethanation activity under both strictly anaerobic and microaerophilic conditions. Evolution of output gas flows methane production (A), pH, total TVFAs and acetate concentration (B), and effluent gas composition (C). The production capacity is indicated as $L.CH_4/Lr/day$. The systematic errors for pH and gas flow measurements were ± 0.01 pH and ± 0.1 mL, respectively. The theoretical minimum flow out is depicted with a green dashed line, whereas the three experimental stages are separated by gray vertical dashed lines. Days of DNA sampling were highlighted in panel 2A. (For interpretation of the references to colour in this figure legend, the reader is referred to the web version of this article.)

SAOB [47]. Among them, three are worth to be mentioned due to their increase in abundance under H_2S exposure. Specifically, Limnochordia sp. DTU66, *Proteinivoracia* sp. DTU68, and Firmicutes sp. DTU69 have almost all the enzymes of the recently proposed alternative WL pathway [48] (**Supplementary Table S5**), thus, are potentially able to establish facultative syntrophic interactions with *Methanobacterium* species.

Third, the capability to process H_2S and other sulfur-based compounds was inspected, since the presence of H_2S in the gas source negatively impacted some of the dominant microbes in S1. Sulfur metabolism is represented by seven modules in the KEGG database [32]. The prevalence of the sulfate/sulfur transport system (M00616) was noteworthy, with almost half of the MAGs encoding the ABC-type sulfate transporter (CysPUWA) (Fig. 3**B**). Similarly, the majority of MAGs showed a completeness of at least 50 % in the biogenesis of Cys (M00021), Met (M00003), and molybdenum cofactor (M00880). In contrast, the metabolic modules related to the oxidation of sulfur-based compounds were much more scattered, as they are associated only with highly specialized microorganisms. The gene *sqr*, responsible for the conversion of H_2S into polysulfide, was observed to be widespread in the community. However, only Gammaproteobacteria sp. DTU53, *Hydrogenophaga* sp. DTU46 and *Burkholderiaceae* sp. DTU134, encoded the sulfide-cytochrome-c reductase (*fccB*, *fccA*) which can process the H_2S into organic sulfur (Fig. 3**C**). Moreover, the presence of thiosulfate sulfurtransferase (*TST*) revealed their role in catalyzing the conversion of sulfide to thiosulfate (**Supplementary Table S6**). The latter can be assimilated into Cys through two sequential enzymatic reactions or processed by the Sox system [49] into sulfate. The thiosulfate oxidation pathway (M00595) exhibited an 80 % completeness level in several MAGs, including *Hydrogenophaga* sp. DTU46 and Gammaproteobacteria sp. DTU53 (Fig. 3**B**). As last remark, Gammaproteobacteria sp. DTU53 emerged as the sole MAG with a complete dissimilatory pathway (M00596), which allows it to use sulfur-containing compounds as electron donors for energy generation (Fig. 3**B**).

3.3. Strain dynamics in the microbiome under selective pressure

Assessing species dynamics alone is not sufficient to comprehend the intricate changes occurring within complex microbiota [11]. To date, this level of investigation has not been conducted on any anaerobic digestion microbiome either, especially with a combined approach

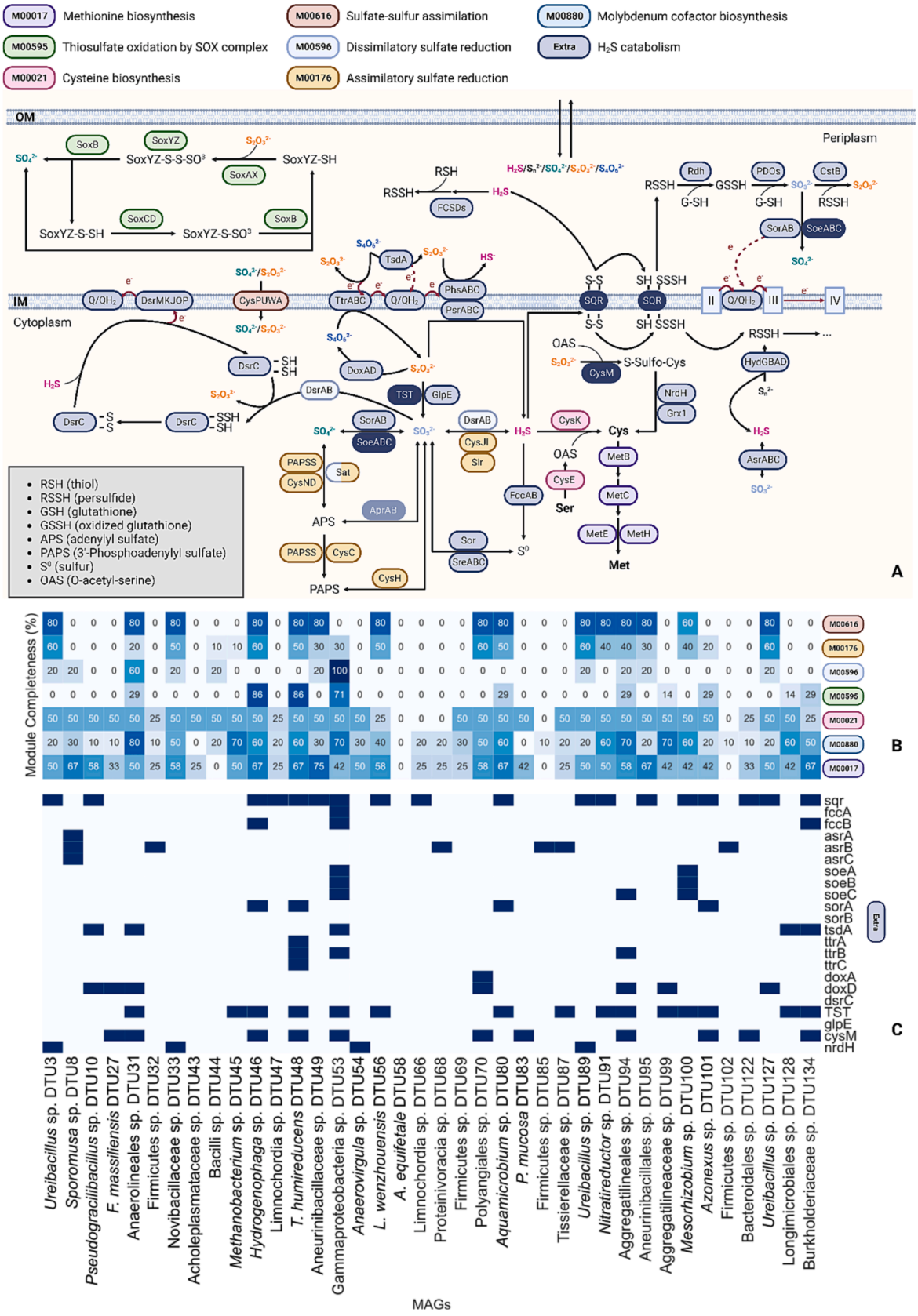

Fig. 3. Sulfur metabolic potential of the microbial community. (**A**) Metabolic map of the sulfur metabolism in gram-negative bacteria. Non-synonymous SNVs were found in the highlighted genes (dark blue, dark yellow) for Gammaproteobacteria sp. DTU53. (**B**) Heatmap representing completeness level (reported as a percentage) of KEGG modules and (**C**) presence (in blue) of some relevant genes in the genomes. The analysis refers to the MAGs presented in Fig. 1. (For interpretation of the references to colour in this figure legend, the reader is referred to the web version of this article.)

employing both variant calling and strain deconvolution. A total of 171,545 unique SNVs were detected across the six samples, 37 % of which were nonsynonymous (nsSNVs). The evolution of strains belonging to the dominant species was tracked by analyzing the shift of nsSNVs frequency over the three experimental stages. Subsequently, to unveil their potential functional impact, nsSNVs were investigated in respect to the affected pathway and the protein structure. Results revealed substantial genetic differences in the MAGs, with species having fluctuating patterns in the occurring variants, while others remained relatively unchanged. Specifically, during S2, a shift in the microbial distribution due to abundance changes at strain-level was observed, with some species showing a severe decrease in the number of detectable variants (**Supplementary Fig. S5**). On the contrary, other species, such as Gammaproteobacteria sp. DTU53 and Limnochordia sp. DTU66, showed an increase in the number of variants.

The phasing of nsSNVs in Gammaproteobacteria sp. DTU53 revealed two distinct clusters. The first had a high frequency during S2, while the second started at low frequency (below 0.2) and increased in S3 (Fig. 4**A, 4C**). Strain deconvolution results mirrored the same patterns (Fig. 4**B, 4D**). Gammaproteobacteria sp. DTU53 was represented by two strains: "str1″ was dominating S2 in both sampling points, while "str0″ rapidly increased in abundance during S3. This shift in abundance is potentially associated with strain str0 having a metabolic advantage over str1 after the injection of air. The other highly abundant microbes were also examined, however no major shift in the strain composition was observed. In particular, either there was only one strain detected, or the dominant strain remained the same throughout the different stages, as for *Methanobacterium* sp. DTU45 and *Hydrogenophaga* sp. DTU46 (**Supplementary Fig. S6**).

The putative impact of nsSNVs on the function of relevant proteins was investigated for Gammaproteobacteria sp. DTU53. More specifically, the nsSNVs having an increased frequency at stages S2 and S3 were mapped on predicted ORFs. Out of 785 and 1375 positively selected nsSNVs for the top and middle part of the reactor, 1–2 % of them were linked to genes involved in the sulfur metabolism, already mentioned in Paragraph 2.2 (Fig. 3**A**). An enrichment of nsSNVs after stage S1 on genes associated with H_2S catabolism was found, even though not statistically significant ($p = 0.137$). Three key enzymes carrying nsSNVs were identified: the A subunits of both adenylylsulfate reductase (*aprA*), sulfite:quinone oxidoreductase (*soeA*) and, sulfide: quinone oxidoreductase (*sqr*). To delve into more detail, a comparison of the predicted 3D structures of the original and mutated SQR was manually inspected and revealed that two nsSNVs had a crucial localization in the protein (Fig. 4**E**). The amino acid change potentially more relevant is the "S292P" variant, where the serine is replaced by a proline. This aa is known to have a higher rigidity due to a much lower solubility (1.54 for S and 36.2 for P) and higher hydrophobicity [50]. The new physico-chemical properties acquired increase the likelihood of the variant to be impacting the structural conformation of the region. To understand if the mutation was located in key regions for the protein functionality, including catalytic sites and binding domains, the sequence was compared with the Swiss-Prot database. A substrate-binding site was identified for SQR in multiple species, including *Aquifex aeolicus*, Acidianus *ambivalens* and *Acidithiobacillus ferrooxidans*, respectively at position V294, D307 and I302 (**Supplementary Fig. S6**) [51–53]. This site is particularly relevant since the conservation of V294 was proposed as a shared site among diverse organisms, where 80 % of the analyzed genes maintained this specific amino acid residue [54]. Therefore, it is possible to speculate that, since S292P is located close to this site, the mutation may have affected its functionality in binding the H_2S molecule.

4. Discussion

The microcosm was affected by changes in input gas source, evidenced by fluctuations in indicators of biomethanation efficiency (Fig. 2). Moreover, as suggested for a similar experimental setup [38], distinct alterations in the composition and structure of the microbial community showed that the feeding strategy exerted a more pronounced selective pressure than the operational gradients present across the height of the TBR (**Supplementary Fig. S2**). The system demonstrated robust biomethanation at the end of each stage, placing it on par with

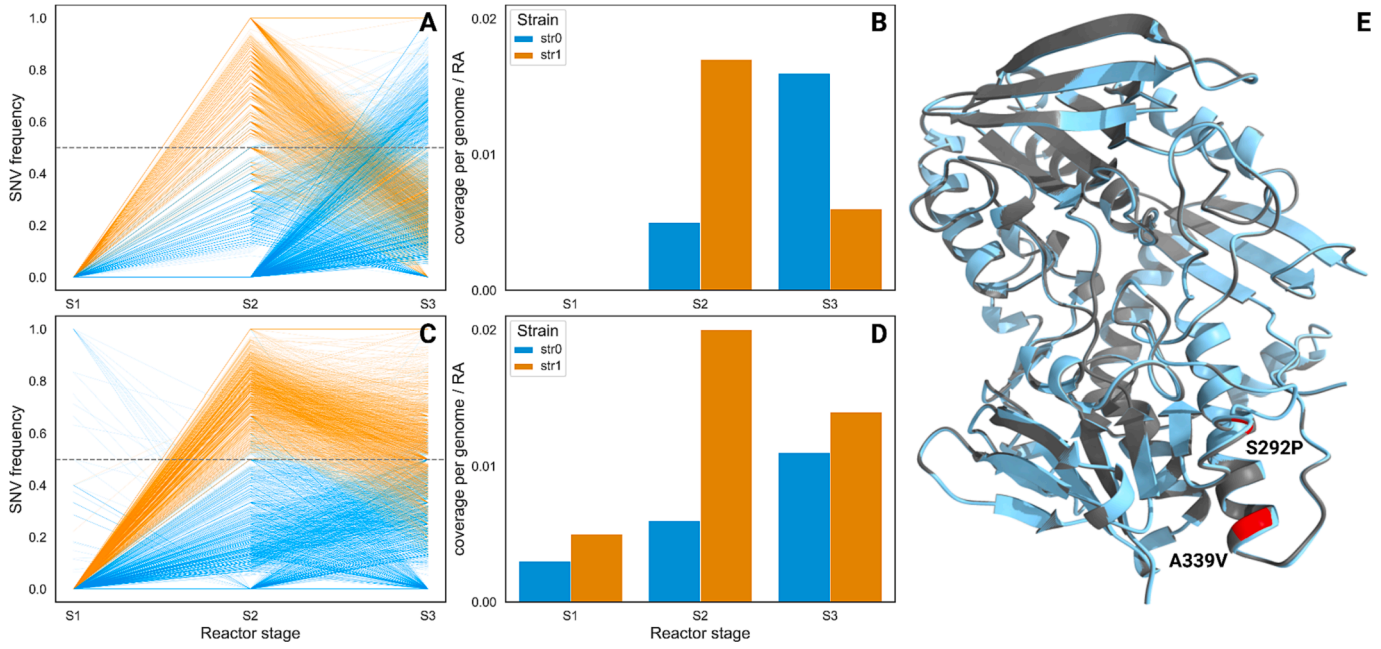

Fig. 4. Frequency of nsSNVs over time and strain deconvolution results for Gammaproteobacteria sp. DTU53. (A, C) SNVs frequency and (B, D) strains relative abundance at different stages and sampling points (top: A, B and middle: C, D). Strain abundances were weighted by species RA and the average value for the three phases was reported. (E) The 3D structures of both the original SQR (in gray) and the one with the variants (in blue) were modeled using AlphaFold[36] and aligned. The SNVs are highlighted in red and reported as: old amino acid + position + new amino acid. (For interpretation of the references to colour in this figure legend, the reader is referred to the web version of this article.)

other TBRs studies for BU [38]. Notably, the average CH_4 concentrations exceed > 95 % over the last 6 days of S1 and across all S3. The biological desulfurization process was effectively implemented, achieving an 81 % removal of H_2S in S3. This removal efficiency aligns closely with values reported in comparable studies involving co-cultures for the co-treatment of CO_2 reduction and H_2S oxidation at mesophilic conditions [8]. From S1 to S2, the methanogenic activity decreased after the addition of H_2S, which, in contrast, favored the growth of H_2S-tolerant bacteria. Furthermore, the dominance shifted from homoacetogenic to SAOB, probably due to the inhibitory effect of high pH and H_2S concentrations on acetate metabolism [42]. The stress caused by H_2S on the methanogen was primarily mitigated by the increased relative abundance of Gammaproteobacteria sp. DTU53 and then further reduced as a result of the air injection in S3. Indeed, based on the functional analysis, Gammaproteobacteria sp. DTU53 emerged as a potential chemotrophic sulfur-oxidizer (Fig. 3). A complete dissimilatory sulfate-reducing pathway enables the microbe to use sulfane sulfur as an electron donor for energy generation [7]. Previous evidence indicated that *Desulfurivibrio alkaliphilus*, possessing the dissimilatory pathway, efficiently supported its growth through the oxidation of sulfide to sulfur [55]. Moreover, Gammaproteobacteria associated species were proposed as SOB [55]. This MAG is potentially able to catalyze the initial oxidative steps via the sulfide-cytochrome-c reductase (*fccB*, *fccA*), that drives the conversion of H_2S into sulfur, or through *sqr,* that oxidizes H_2S into polysulfide (Fig. 3**A**) [54]. Therefore, given the extensive sulfur-related metabolic potential of the MAG and its response following H_2S supplementation, it was assigned a pivotal role in the desulfurization process. A multi-process role of Gammaproteobacteria sp. DTU53 in the system was also hypothesized. Indeed, together with *Hydrogenophaga* sp. DTU46 and *Burkholderiaceae* sp. DTU134, it possessed a nearly complete alternative WL pathway [48], allowing the establishment of syntrophic interaction with the archaeon (Fig. 5). The introduction of O_2 in S3 had negligible effects on the activity of *Methanobacterium* sp. DTU45 or on the putative SOB. As previously suggested [38,40,56], the ability of *Methanobacterium* to form biofilms presumably served as protection against toxic agents, including O_2 [46]. Moreover, functional annotations revealed that the formation of a mature biofilm was a multispecies process involving also Gammaproteobacteria sp. DTU53 and *Hydrogenophaga* sp. DTU46 (Fig. 5).

Despite the protection provided by the biofilm, the changes in gas streams exerted a strong selective pressure, acting at multiple levels. In general, both species and strain level substitution occur after a stress and the establishment of a new equilibrium, as already seen for the gut microbiome [11]. The increased abundance of Gammaproteobacteria sp. DTU53 in S2 can be attributed to the more favorable conditions, meeting the species metabolism to exploit the available energetic substrates. However, the adaptation and resilience of Gammaproteobacteria sp. DTU53 to the stresses is likely associated with strains selection ("str0" and "str1"). Differences in fitness among strains are due to the accumulation of genomic variants providing a phenotypic advantage. Here, strain-level deconvolution unveiled a remarkable intra-species diversity, wherein two coexisting strains exhibited distinct phenotypes, as evidenced by their varying responses to O_2. This observation suggested that strains may contribute to an additional layer of functional redundancy within the microbiome. The shift observed between "str0" and "str1" resulted in a more pronounced change in the top layer. The upper part is closer to the gas inlet, thus where the O_2 partial pressure is expected to be the highest [38]. Therefore, it is possible that the positive selection of "str0" may be directly or indirectly related to the O_2 metabolism, such as resistance mechanisms. A deeper investigation of the nsSNVs mapping to coding regions in sulfur metabolism showed two mutations on the gene *sqr* in "str0". The encoded SQR is located in the peripheral membrane where it plays a role in sulfide detoxification and its use as an energetic source. SQR catalyzes the oxidation of sulfide to elemental sulfur by transferring electrons to the quinone pool in the membrane, leading to ATP synthesis by an electrochemical gradient

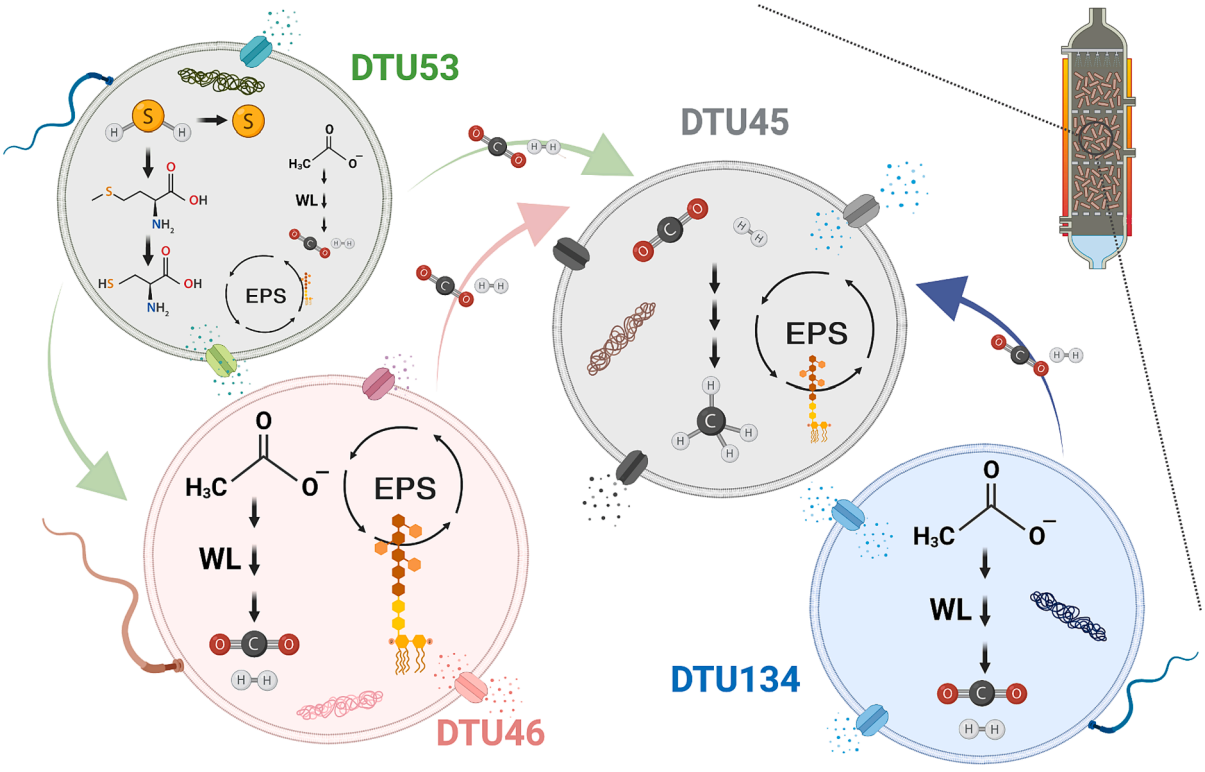

Fig. 5. Schematic interactions occurring among the dominant microbes. The main metabolic functions were represented for *Methanobacterium* sp. DTU45, *Burkholderiaceae* sp. DTU134, Gammaproteobacteria sp. DTU53 and *Hydrogenophaga* sp. DTU46. Specific focus was posed on hydrogenotrophic methanogenesis, WL pathway, EPS secretion and H_2S catabolism.

across the membrane [54]. Both variants identified (A339V and S292P) were nonsynonymous, thus affecting the amino acid composition. Specifically, the replacement of serine with proline, holds greater significance due to its possible consequences on the structure flexibility. Indeed, the affected portion of SQR is in proximity to the FAD binding site, previously identified as V294 in a crystallographic study of *A. aeolicus* [53]. V294 is the amino acid located at the entrance of the channel allowing sulfide to access the catalytic site, and as previously demonstrated, it is essential for the activity of the enzyme [57]. Therefore, the identified mutation could be hypothesized to have impacted the protein functionality by potentially increasing its affinity for sulfide or facilitating sulfide entry. This alteration could have conferred a phenotypic advantage to the strain carrying it, elucidating the observed shift in dominance (Fig. 4**B,4D**).

Overall, this study demonstrated that coupling biomethanation and desulfurization in microaerophilic conditions ensures effective H_2S removal without inhibiting the activity of hydrogenotrophic archaea. In a concluding assessment of considerable significance, strain-specific analysis emphasizes the importance of genetic variability on intracellular mechanisms and bioenergetic pathways. Strain-level resolution becomes to elucidate the effect of selective pressures, which profoundly influence microbial community architectures and configuration.

CRediT authorship contribution statement

Gabriele Ghiotto: Writing – review & editing, Writing – original draft, Visualization, Software, Methodology, Formal analysis, Data curation, Conceptualization. **Nicola De Bernardini:** Writing – review & editing, Writing – original draft, Visualization, Software, Methodology, Investigation, Formal analysis, Data curation. **Ginevra Giangeri:** Writing – original draft, Methodology, Investigation, Data curation. **Panagiotis Tsapekos:** Methodology, Investigation, Data curation, Conceptualization. **Maria Gaspari:** Methodology, Investigation, Data curation. **Panagiotis G. Kougias:** Methodology, Investigation, Data curation, Conceptualization. **Stefano Campanaro:** Writing – review & editing, Supervision. **Irini Angelidaki:** Writing – review & editing, Supervision, Resources, Funding acquisition, Conceptualization. **Laura Treu:** Writing – review & editing, Supervision, Resources, Funding acquisition, Conceptualization.

Declaration of competing interest

The authors declare that they have no known competing financial interests or personal relationships that could have appeared to influence the work reported in this paper.

Data availability

Data will be made available on request.

Acknowledgements

This work was financially supported by the projects “SEMPRE-BIO - HORIZON-CL5-2021-D3-03” (Project ID 101084297) and LIFE20 CCM/GR/001642 - LIFE CO2toCH4 of the European Union LIFE + program. Additionally, support was also provided by the project “Harnessing potential of biological CO2 capture for Circular Economy” (CooCE) (Project No 327331) which is co-funded by the European Commission (receiving funding from European Union’s Horizon 2020 Grant agreement No. 691712) and national funds (Ministero dell’Università e Ricerca MUR, Italy) under the ERA-Net Cofund ACCELERATING CCS TECHNOLOGIES (ACT).

Data availability.

Raw data from metagenomic and metatranscriptomic analyses generated in this study have been deposited in the NCBI under BioProject number PRJNA972863. Data will be made available on request.

Appendix A. Supplementary data

Supplementary data to this article can be found online at https://doi.org/10.1016/j.cej.2024.149824.

References

[1] I. Angelidaki, L. Treu, P. Tsapekos, G. Luo, S. Campanaro, H. Wenzel, P.G. Kougias, Biogas upgrading and utilization: Current status and perspectives, Biotechnol. Adv. 36 (2018) 452–466, https://doi.org/10.1016/j.biotechadv.2018.01.011.
[2] H. Huynh Nhut, V. Le Thi Thanh, L. Tran Le, Removal of H2S in biogas using biotrickling filter: Recent development, Process Saf, Environ. Prot. 144 (2020) 297–309, https://doi.org/10.1016/j.psep.2020.07.011.
[3] L. Deng, Y. Liu, W. Wang, in: Biogas Cleaning and Upgrading, Biogas Technol., Springer, Singapore, 2020, pp. 201–243, https://doi.org/10.1007/978-981-15-4940-3_6.
[4] D. Pokorna, J. Zabranska, Sulfur-oxidizing bacteria in environmental technology, Biotechnol. Adv. 33 (2015) 1246–1259, https://doi.org/10.1016/j.biotechadv.2015.02.007.
[5] J. You, J. Chen, Y. Sun, J. Fang, Z. Cheng, J. Ye, D. Chen, Treatment of mixed waste-gas containing H2S, dichloromethane and tetrahydrofuran by a multi-layer biotrickling filter, J. Clean. Prod. 319 (2021) 128630, https://doi.org/10.1016/j.jclepro.2021.128630.
[6] J. Wang, F. Xue, Z. Cheng, J. Wang, D. Chen, J. Zhao, S. Qiu, Temperature and pH on microbial desulfurization of sulfide wastewater: From removal performance to gene regulation mechanism, J. Water Process Eng. 53 (2023) 103720, https://doi.org/10.1016/j.jwpe.2023.103720.
[7] S. Neukirchen, I.A.C. Pereira, F.L. Sousa, Stepwise pathway for early evolutionary assembly of dissimilatory sulfite and sulfate reduction, ISME J. (2023) 1–13, https://doi.org/10.1038/s41396-023-01477-y.
[8] T.L. Dupnock, M.A. Deshusses, Biological Co-treatment of H2S and reduction of CO2 to methane in an anoxic biological trickling filter upgrading biogas, Chemosphere 256 (2020) 127078, https://doi.org/10.1016/j.chemosphere.2020.127078.
[9] J.V. Henkel, O. Dellwig, F. Pollehne, D.P.R. Herlemann, T. Leipe, H.N. Schulz-Vogt, A bacterial isolate from the Black Sea oxidizes sulfide with manganese(IV) oxide, Proc. Natl. Acad. Sci. U. S. A. 116 (2019) 12153–12155, https://doi.org/10.1073/pnas.1906000116.
[10] J. Wang, Z. Cheng, J. Wang, D. Chen, J. Chen, J. Yu, S. Qiu, D.D. Dionysiou, Enhancement of bio-S0 recovery and revealing the inhibitory effect on microorganisms under high sulfide loading, Environ. Res. 238 (2023) 117214, https://doi.org/10.1016/j.envres.2023.117214.
[11] M. Roodgar, B.H. Good, N.R. Garud, S. Martis, M. Avula, W. Zhou, S.M. Lancaster, H. Lee, A. Babveyh, S. Nesamoney, K.S. Pollard, M.P. Snyder, Longitudinal linked-read sequencing reveals ecological and evolutionary responses of a human gut microbiome during antibiotic treatment, Genome Res. 31 (2021) 1433–1446, https://doi.org/10.1101/gr.265058.120.
[12] L. Bucci, G. Ghiotto, G. Zampieri, R. Raga, L. Favaro, L. Treu, S. Campanaro, Adaptation of Anaerobic Digestion Microbial Communities to High Ammonium Levels: Insights from Strain-Resolved Metagenomics, Environ. Sci. Technol. (2023), https://doi.org/10.1021/acs.est.3c07737.
[13] M.L.B. Celis-García, F. Ramírez, S. Revah, E. Razo-Flores, O. Monroy, Sulphide and Oxygen Inhibition over the Anaerobic Digestion of Organic Matter: Influence of Microbial Immobilization Type, Environ. Technol. 25 (2004) 1265–1275, https://doi.org/10.1080/09593332508618367.
[14] L. Treu, P.G. Kougias, B. de Diego-Díaz, S. Campanaro, I. Bassani, J. Fernández-Rodríguez, I. Angelidaki, Two-year microbial adaptation during hydrogen-mediated biogas upgrading process in a serial reactor configuration, Bioresour. Technol. 264 (2018) 140–147, https://doi.org/10.1016/j.biortech.2018.05.070.
[15] V.B. Centurion, A. Rossi, E. Orellana, G. Ghiotto, B. Kakuk, M.S. Morlino, A. Basile, G. Zampieri, L. Treu, S. Campanaro, A unified compendium of prokaryotic and viral genomes from over 300 anaerobic digestion microbiomes, Environ. Microbiome 19 (2024) 1, https://doi.org/10.1186/s40793-023-00545-2.
[16] M.R. Olm, A. Crits-Christoph, K. Bouma-Gregson, B.A. Firek, M.J. Morowitz, J. F. Banfield, inStrain profiles population microdiversity from metagenomic data and sensitively detects shared microbial strains, Nat. Biotechnol. 39 (2021) 727–736, https://doi.org/10.1038/s41587-020-00797-0.
[17] C. Quince, S. Nurk, S. Raguideau, R. James, O.S. Soyer, J.K. Summers, A. Limasset, A.M. Eren, R. Chikhi, A.E. Darling, STRONG: metagenomics strain resolution on assembly graphs, Genome Biol. 22 (2021) 214, https://doi.org/10.1186/s13059-021-02419-7.
[18] L. Treu, P. Tsapekos, M. Peprah, S. Campanaro, A. Giacomini, V. Corich, P. G. Kougias, I. Angelidaki, Microbial profiling during anaerobic digestion of cheese whey in reactors operated at different conditions, Bioresour. Technol. 275 (2019) 375–385, https://doi.org/10.1016/j.biortech.2018.12.084.
[19] G. Zampieri, S. Campanaro, C. Angione, L. Treu, Metatranscriptomics-guided genome-scale metabolic modeling of microbial communities, Cell Rep. Methods 3 (2023) 100383, https://doi.org/10.1016/j.crmeth.2022.100383.
[20] A.M. Bolger, M. Lohse, B. Usadel, Trimmomatic: a flexible trimmer for Illumina sequence data, Bioinformatics 30 (2014) 2114–2120, https://doi.org/10.1093/bioinformatics/btu170.
[21] D. Li, C.-M. Liu, R. Luo, K. Sadakane, T.-W. Lam, MEGAHIT: an ultra-fast single-node solution for large and complex metagenomics assembly via succinct de Bruijn

graph, Bioinformatics 31 (2015) 1674–1676, https://doi.org/10.1093/bioinformatics/btv033.
[22] B. Langmead, S.L. Salzberg, Fast gapped-read alignment with Bowtie 2, Nat. Methods 9 (2012) 357–359, https://doi.org/10.1038/nmeth.1923.
[23] A. Chklovski, D.H. Parks, B.J. Woodcroft, G.W. Tyson, CheckM2: a rapid, scalable and accurate tool for assessing microbial genome quality using machine learning, (2022) 2022.07.11.499243. https://doi.org/10.1101/2022.07.11.499243.
[24] C.M.K. Sieber, A.J. Probst, A. Sharrar, B.C. Thomas, M. Hess, S.G. Tringe, J. F. Banfield, Recovery of genomes from metagenomes via a dereplication, aggregation and scoring strategy, Nat. Microbiol. 3 (2018) 836–843, https://doi.org/10.1038/s41564-018-0171-1.
[25] R.M. Bowers, N.C. Kyrpides, R. Stepanauskas, M. Harmon-Smith, D. Doud, T.B. K. Reddy, F. Schulz, J. Jarett, A.R. Rivers, E.A. Eloe-Fadrosh, S.G. Tringe, N. N. Ivanova, A. Copeland, A. Clum, E.D. Becraft, R.R. Malmstrom, B. Birren, M. Podar, P. Bork, G.M. Weinstock, G.M. Garrity, J.A. Dodsworth, S. Yooseph, G. Sutton, F.O. Glöckner, J.A. Gilbert, W.C. Nelson, S.J. Hallam, S.P. Jungbluth, T. J.G. Ettema, S. Tighe, K.T. Konstantinidis, W.-T. Liu, B.J. Baker, T. Rattei, J. A. Eisen, B. Hedlund, K.D. McMahon, N. Fierer, R. Knight, R. Finn, G. Cochrane, I. Karsch-Mizrachi, G.W. Tyson, C. Rinke, A. Lapidus, F. Meyer, P. Yilmaz, D. H. Parks, A. Murat Eren, L. Schriml, J.F. Banfield, P. Hugenholtz, T. Woyke, Minimum information about a single amplified genome (MISAG) and a metagenome-assembled genome (MIMAG) of bacteria and archaea, Nat. Biotechnol. 35 (2017) 725–731, https://doi.org/10.1038/nbt.3893.
[26] P.-A. Chaumeil, A.J. Mussig, P. Hugenholtz, D.H. Parks, GTDB-Tk v2: memory friendly classification with the genome taxonomy database, Bioinformatics 38 (2022) 5315–5316, https://doi.org/10.1093/bioinformatics/btac672.
[27] F. Asnicar, A.M. Thomas, F. Beghini, C. Mengoni, S. Manara, P. Manghi, Q. Zhu, M. Bolzan, F. Cumbo, U. May, J.G. Sanders, M. Zolfo, E. Kopylova, E. Pasolli, R. Knight, S. Mirarab, C. Huttenhower, N. Segata, Precise phylogenetic analysis of microbial isolates and genomes from metagenomes using PhyloPhlAn 3.0, Nat. Commun. 11 (2020) 2500, https://doi.org/10.1038/s41467-020-16366-7.
[28] I. Letunic, P. Bork, Interactive Tree Of Life (iTOL) v5: an online tool for phylogenetic tree display and annotation, Nucleic Acids Res. 49 (2021) W293–W296, https://doi.org/10.1093/nar/gkab301.
[29] B.J. Woodcroft, CoverM, (2023). https://github.com/wwood/CoverM (accessed March 30, 2023).
[30] D. Hyatt, G.-L. Chen, P.F. LoCascio, M.L. Land, F.W. Larimer, L.J. Hauser, Prodigal: prokaryotic gene recognition and translation initiation site identification, BMC Bioinformatics 11 (2010) 119, https://doi.org/10.1186/1471-2105-11-119.
[31] C.P. Cantalapiedra, A. Hernández-Plaza, I. Letunic, P. Bork, J. Huerta-Cepas, eggNOG-mapper v2: Functional Annotation, Orthology Assignments, and Domain Prediction at the Metagenomic Scale, Mol. Biol. Evol. 38 (2021) 5825–5829, https://doi.org/10.1093/molbev/msab293.
[32] M. Kanehisa, M. Furumichi, Y. Sato, M. Kawashima, M. Ishiguro-Watanabe, KEGG for taxonomy-based analysis of pathways and genomes, Nucleic Acids Res. 51 (2023) D587–D592, https://doi.org/10.1093/nar/gkac963.
[33] C.A. Ruiz-Perez, R.E. Conrad, K.T. Konstantinidis, MicrobeAnnotator: a user-friendly, comprehensive functional annotation pipeline for microbial genomes, BMC Bioinformatics 22 (2021) 11, https://doi.org/10.1186/s12859-020-03940-5.
[34] G. Ghiotto, G. Zampieri, S. Campanaro, L. Treu, Strain-resolved metagenomics approaches applied to biogas upgrading, Environ. Res. (2023) 117414, https://doi.org/10.1016/j.envres.2023.117414.
[35] M. Mirdita, K. Schütze, Y. Moriwaki, L. Heo, S. Ovchinnikov, M. Steinegger, ColabFold: making protein folding accessible to all, Nat. Methods 19 (2022) 679–682, https://doi.org/10.1038/s41592-022-01488-1.
[36] J. Jumper, R. Evans, A. Pritzel, T. Green, M. Figurnov, O. Ronneberger, K. Tunyasuvunakool, R. Bates, A. Žídek, A. Potapenko, A. Bridgland, C. Meyer, S.A. A. Kohl, A.J. Ballard, A. Cowie, B. Romera-Paredes, S. Nikolov, R. Jain, J. Adler, T. Back, S. Petersen, D. Reiman, E. Clancy, M. Zielinski, M. Steinegger, M. Pacholska, T. Berghammer, S. Bodenstein, D. Silver, O. Vinyals, A.W. Senior, K. Kavukcuoglu, P. Kohli, D. Hassabis, Highly accurate protein structure prediction with AlphaFold, Nature 596 (2021) 583–589, https://doi.org/10.1038/s41586-021-03819-2.
[37] M.A. Larkin, G. Blackshields, N.P. Brown, R. Chenna, P.A. McGettigan, H. McWilliam, F. Valentin, I.M. Wallace, A. Wilm, R. Lopez, J.D. Thompson, T. J. Gibson, D.G. Higgins, Clustal W and Clustal X version 2.0, Bioinforma, Oxf. Engl. 23 (2007) 2947–2948, https://doi.org/10.1093/bioinformatics/btm404.
[38] F. Ebrahimian, N. De Bernardini, P. Tsapekos, L. Treu, X. Zhu, S. Campanaro, K. Karimi, I. Angelidaki, Effect of pressure on biomethanation process and spatial stratification of microbial communities in trickle bed reactors under decreasing gas retention time, Bioresour. Technol. 361 (2022) 127701, https://doi.org/10.1016/j.biortech.2022.127701.
[39] F.B. Sarmiento, J.A. Leigh, W.B. Whitman, Chapter three - Genetic Systems for Hydrogenotrophic Methanogens, in: A.C. Rosenzweig, S.W. Ragsdale (Eds.), Methods Enzymol, Academic Press, 2011, pp. 43–73, https://doi.org/10.1016/B978-0-12-385112-3.00003-2.
[40] P. Tsapekos, L. Treu, S. Campanaro, V.B. Centurion, X. Zhu, M. Peprah, Z. Zhang, P. G. Kougias, I. Angelidaki, Pilot-scale biomethanation in a trickle bed reactor: Process performance and microbiome functional reconstruction, Energy Convers. Manag. 244 (2021) 114491, https://doi.org/10.1016/j.enconman.2021.114491.
[41] Z. Xie, S. Huang, Y. Wan, F. Deng, Q. Cao, X. Liu, D. Li, Power to biogas upgrading: Effects of different H2/CO2 ratios on products and microbial communities in anaerobic fermentation system, Sci. Total Environ. 865 (2023) 161305, https://doi.org/10.1016/j.scitotenv.2022.161305.
[42] E. Ntagia, I. Chatzigiannidou, A.J. Williamson, J.B.A. Arends, K. Rabaey, Homoacetogenesis and microbial community composition are shaped by pH and total sulfide concentration, Microb. Biotechnol. 13 (2020) 1026–1038, https://doi.org/10.1111/1751-7915.13546.
[43] H. Kirchhoff, Acholeplasma equifetale and Acholeplasma hippikon, Two New Species from Aborted Horse Fetuses, Int. J. Syst. Bacteriol. 28 (1978) 76–81, https://doi.org/10.1099/00207713-28-1-76.
[44] D. Ruan, Z. Zhou, H. Pang, J. Yao, G. Chen, Z. Qiu, Enhancing methane production of anaerobic sludge digestion by microaeration: Enzyme activity stimulation, semi-continuous reactor validation and microbial community analysis, Bioresour. Technol. 289 (2019) 121643, https://doi.org/10.1016/j.biortech.2019.121643.
[45] C. Wu, Y. Zhou, P. Wang, S. Guo, Improving hydrolysis acidification by limited aeration in the pretreatment of petrochemical wastewater, Bioresour. Technol. 194 (2015) 256–262, https://doi.org/10.1016/j.biortech.2015.06.072.
[46] J.A. Magdalena, L.T. Angenent, J.G. Usack, The Measurement, application, and effect of oxygen in microbial fermentations: focusing on methane and carboxylate production, Fermentation 8 (2022) 138, https://doi.org/10.3390/fermentation8040138.
[47] S. Dyksma, L. Jansen, C. Gallert, Syntrophic acetate oxidation replaces acetoclastic methanogenesis during thermophilic digestion of biowaste, Microbiome 8 (2020) 105, https://doi.org/10.1186/s40168-020-00862-5.
[48] M.K. Nobu, T. Narihiro, C. Rinke, Y. Kamagata, S.G. Tringe, T. Woyke, W.-T. Liu, Microbial dark matter ecogenomics reveals complex synergistic networks in a methanogenic bioreactor, ISME J. 9 (2015) 1710–1722, https://doi.org/10.1038/ismej.2014.256.
[49] Y. Kawano, K. Suzuki, I. Ohtsu, Current understanding of sulfur assimilation metabolism to biosynthesize l-cysteine and recent progress of its fermentative overproduction in microorganisms, Appl. Microbiol. Biotechnol. 102 (2018) 8203–8211, https://doi.org/10.1007/s00253-018-9246-4.
[50] D.L. Nelson, M.M. Cox, Lehninger Principles of Biochemistry, Freeman, W. H, 2017.
[51] J.A. Brito, F.L. Sousa, M. Stelter, T.M. Bandeiras, C. Vonrhein, M. Teixeira, M. M. Pereira, M. Archer, Structural and functional insights into sulfide:quinone oxidoreductase, Biochemistry 48 (2009) 5613–5622, https://doi.org/10.1021/bi9003827.
[52] M.M. Cherney, Y. Zhang, M.N.G. James, J.H. Weiner, Structure-activity characterization of sulfide:quinone oxidoreductase variants, J. Struct. Biol. 178 (2012) 319–328, https://doi.org/10.1016/j.jsb.2012.04.007.
[53] M. Marcia, U. Ermler, G. Peng, H. Michel, The structure of Aquifex aeolicus sulfide: quinone oxidoreductase, a basis to understand sulfide detoxification and respiration, Proc. Natl. Acad. Sci. 106 (2009) 9625–9630, https://doi.org/10.1073/pnas.0904165106.
[54] F.M. Sousa, J.G. Pereira, B.C. Marreiros, M.M. Pereira, Taxonomic distribution, structure/function relationship and metabolic context of the two families of sulfide dehydrogenases: SQR and FCSD, Biochim. Biophys. Acta BBA - Bioenerg. 2018 (1859) 742–753, https://doi.org/10.1016/j.bbabio.2018.04.004.
[55] C. Thorup, A. Schramm, A.J. Findlay, K.W. Finster, L. Schreiber, Disguised as a Sulfate Reducer: Growth of the Deltaproteobacterium Desulfurivibrio alkaliphilus by Sulfide Oxidation with Nitrate, mBio 8 (2017) e00671-17. https://doi.org/10.1128/mBio.00671-17.
[56] N. De Bernardini, A. Basile, G. Zampieri, A. Kovalovszki, B. De Diego Diaz, E. Offer, N. Wongfaed, I. Angelidaki, P.G. Kougias, S. Campanaro, L. Treu, Integrating metagenomic binning with flux balance analysis to unravel syntrophies in anaerobic CO2 methanation, Microbiome 10 (2022) 117, https://doi.org/10.1186/s40168-022-01311-1.
[57] C. Griesbeck, M. Schütz, T. Schödl, S. Bathe, L. Nausch, N. Mederer, M. Vielreicher, G. Hauska, Mechanism of Sulfide-Quinone Reductase Investigated Using Site-Directed Mutagenesis and Sulfur Analysis, Biochemistry 41 (2002) 11552–11565, https://doi.org/10.1021/bi026032b.